# The effect of natural convection on solidification in tall tapered feeders

C. H. Li* D. R. Jenkins†

(Received 30 September 2002)

**Abstract**

Tall tapered feeders (TTFs) are used in foundry casting to supply additional molten metal to a casting, in order to overcome problems associated with shrinkage upon freezing. Due to the shape and volume of TTFs, natural convection may play a significant role in heat transfer and hence affect the progress of the solidification front. A computational model of heat transfer and fluid flow in a TTF, incorporating natural convection, is presented. The heat equation is solved in terms of temperature, rather than enthalpy. Latent heat is incorporated by an "apparent capacity" formulation. An iterative scheme is used to calculate the latent heat effect using the liquid fraction. Flow in the mushy zone is represented by a Darcy-like resistance term and the Navier-Stokes equations are solved using a modified operator splitting method.

*CSIRO Mathematical and Information Sciences Locked Bag 17, North Ryde 1670, AUSTRALIA. mailto:Chinhsien.Li@csiro.au

†as above. mailto:David.R.Jenkins@csiro.au

[0]See http://anziamj.austms.org.au/V44/CTAC2001/Li00 for this article,
 Published 1 April 2003. ISSN 1446-8735

The approach yields an accurate solution for both flow and temperature fields. The results confirm that solidification progress is affected by convection at early times, after which conduction dominates.

# Contents



# 1 Introduction

A problem associated with the casting of molten iron in sand moulds was presented at the MISG 2001. It concerned the solidification behaviour in tall tapered feeders (TTFs), which are used to supply additional molten metal to a casting to overcome shrinkage within the casting. It became clear that natural convection could play a significant part in the solidification behaviour of TTFs. Many castings have relatively narrow cross-sections, which inhibits the onset and development of natural convection. As a result, natural convection is often not explicitly accounted for in standard computational models of foundry castings [1, 2]. This considerably reduces the cost of

Table 1: notation

| | | | |
|---|---|---|---|
| $\mathbf{u}$ | velocity vector; | $\rho$ | density; |
| $T$ | temperature; | $p$ | pressure; |
| $\nu$ | kinematic viscosity; | $g$ | gravity; |
| $T_r$ | representative temperature; | $\beta$ | thermal expansion coefficient; |
| $g_l$ | liquid fraction; | $K_o$ | Darcy coefficient scale factor; |
| $\tilde{K}$ | coefficient of Darcy force; | $C$ | specific heat; |
| $\hat{C}$ | apparent heat capacity; | $k$ | heat conductivity; |
| $L$ | latent heat of solidification; | $T_s$ | solidus temperature; |
| $T_l$ | liquidus temperature; | $h$ | heat transfer coefficient; |
| $\mathbf{n}$ | unit vector along vertical axis; | $\nabla$ | gradient operator; |
| $\frac{\partial}{\partial n}$ | outward normal derivative. | | |

computation. In some cases, however, natural convection will have some effect, at least during the early period of solidification, which in turn could have consequences for the later solidification progress, such as the effects of shrinkage. This is likely to be the case for TTFs due to their relatively large size. Therefore it is desirable to incorporate natural convection into modelling of solidification in TTFs. The purpose of this work is to describe the development of such a capability and present some sample results.

In the following we present the model equations and describe the numerical solution scheme. We then present results for an example TTF configuration, which show clearly the dominant effect of convection during the early period of solidification, for example, retarding of solidification, and change of the pattern of the solidification front.

# 2 Model equations

Consider the problem in $N$-dimensional space ($N = 2$ or 3) with the vertical axis pointing upward. Assume that the density of the liquid is constant except in the buoyancy term, that is, Boussinesq flow in the casting region, and that the mushy region (the region between solidus and liquidus temperatures) has a columnar structure. Then we have the following governing equations [2, 3, 4, 5, 6].

**Momentum equation:**

$$\frac{\partial \mathbf{u}}{\partial t} + (\mathbf{u}\cdot\nabla)\mathbf{u} - \nabla\cdot(\nu\nabla)\mathbf{u} + \tilde{K}\mathbf{u} + \nabla p = \beta g_l (T - T_r) g\mathbf{n}\,. \quad (1)$$

**Equation of continuity:**

$$\nabla\cdot\mathbf{u} = 0\,, \quad (2)$$

where $\tilde{K} = K_o(1-g_l)^2/g_l^3$, and

$$g_l = \begin{cases} 0\,, & T \le T_s\,; \\ \frac{T-T_s}{T_l-T_s}\,, & T_s < T < T_l\,; \\ 1\,, & T \ge T_l\,. \end{cases}$$

The columnar structure is typical of the solidification of molten metals [3], and flow in such a structure is best represented by a Darcy-like flow resistance term, with coefficient $\tilde{K}$ in the momentum equation (1). The liquid fraction model is a simple linear function of temperature, although other models could equally well have been used.

**Heat equation:**

$$\hat{C}\frac{\partial T}{\partial t} + \rho C(\mathbf{u}\cdot\nabla)T - \nabla\cdot(k\nabla)T = 0\,, \tag{3}$$

where

$$\hat{C} = \begin{cases} \rho C\,, & T \le T_s \text{ or } T \ge T_l\,; \\ \rho C + \rho L\frac{dg_l(T)}{dT}\,, & T_s < T < T_l\,. \end{cases} \tag{4}$$

The boundary condition at the interface with the sand mould of the casting is

$$-k\frac{\partial T}{\partial n} = h(T - T_{\text{sand}})\,,$$

which is meant to represent the flux of heat into a sand mould with a constant temperature $T_{\text{sand}}$.

Note that the latent heat is not included in the advection term in the heat equation, which is a consequence of the columnar model of the mushy layer [3]. The temperature dependence of $g_l$ implies that latent heat is released uniformly across the mushy layer.

In the above equations, all of $k$, $C$, $\nu$ and $h$ are considered to be dependent on the local metal temperature.

# 3 Solution by segregated time stepping

Let $t^n$ be the time at the $n$th step, $\Delta t$ the time step size, and let $f^{n+\eta}$ denote the value at $t = t^n + \eta\,\Delta t$ of the function $f(t)$. From the known solution at $t^n$ obtain the solution at $t^{n+1}$ for

$$\{T^{n+1}, k^{n+1}, C^{n+1}, g_l^{n+1}, \hat{C}^{n+1}, h^{n+1}; \nu^{n+1}, \mathbf{u}^{n+1}, p^{n+1}\}$$

using the segregated time-stepping scheme:

1. Solve for $T^{n+1}$ the heat equation in casting region by backward Euler scheme:

$$\hat{C}^{n+\frac{1}{2}}\frac{T^{n+1}-T^n}{\Delta t}+\rho C^{n+\frac{1}{2}}(\mathbf{u}^n\cdot\nabla)T^{n+1} - \nabla\cdot(k^{n+\frac{1}{2}}\nabla)T^{n+1}=0\,, \tag{5}$$

with boundary condition at the interface with sand mould

$$-k^{n+\frac{1}{2}}\frac{\partial T^{n+1}}{\partial n}=h^{n+\frac{1}{2}}(T^{n+1}-T_{\text{sand}})\,.$$

2. update temperature dependent properties in casting region:

$$k^{n+1}=k(T^{n+1})\,,\quad C^{n+1}=C(T^{n+1})\,,\quad g_l^{n+1}=g_l(T^{n+1})\,,$$
$$\hat{C}^{n+1}=\hat{C}(T^{n+1})\,,\quad h^{n+1}=h(T^{n+1})\,,\quad \nu^{n+1}=\nu(T^{n+1})\,.$$

3. solve for $\{\mathbf{u}^{n+1},p^{n+1}\}$ the Navier-Stokes equation in casting region:

$$\frac{\partial\mathbf{u}}{\partial t}+(\mathbf{u}\cdot\nabla)\mathbf{u}-\nabla\cdot(\nu^{n+1}\nabla)\mathbf{u}+\tilde{K}^{n+1}\mathbf{u}+\nabla p = \beta g_l^{n+1}(T^{n+1}-T_r)g\mathbf{n}\,, \tag{6}$$
$$\nabla\cdot\mathbf{u}=0\,, \tag{7}$$

with $\tilde{K}^{n+1}=\tilde{K}(g_l^{n+1})=K_o(1-g_l^{n+1})^2/(g_l^{n+1})^3$.

The Navier-Stokes equations (6–7) are solved by an operator-splitting scheme [7], while the heat equation (5) is solved by a predictor-corrector iterative scheme in order that the effect of latent heat is correctly accounted for:

Obtain the predictor temperature value $\check{T}$ by solving the semi-discrete heat equation below:

$$\hat{C}^n\frac{\check{T}-T^n}{\Delta t}+\rho C^n(\mathbf{u}^n\cdot\nabla)\check{T}-\nabla\cdot(k^n\nabla)\check{T}=0\,, \tag{8}$$

with the condition at the sand mould interface

$$-k^n \frac{\partial \check{T}}{\partial n} = h^n (\check{T} - T_{\text{sand}}) \,,$$

then apply the following corrector iterations:

1. Let $T^{n+1,0} = \check{T}$. For $l \geq 1$, from $T^{n+1,l-1} \longrightarrow T^{n+1,l}$ as follows:
2. define $T^{n+\frac{1}{2}} = \frac{1}{2}(T^{n+1,l-1} + T^n)$.
3. update

$$k^{n+\frac{1}{2}} = k(T^{n+\frac{1}{2}}) \,, \quad C^{n+\frac{1}{2}} = C(T^{n+\frac{1}{2}}) \,,$$
$$h^{n+\frac{1}{2}} = h(T^{n+\frac{1}{2}}) \,, \quad g_l^{n+1,l-1} = g_l(T^{n+1,l-1}) \,,$$
$$\hat{C}^{n+\frac{1}{2}} = \begin{cases} \rho C^{n+\frac{1}{2}} + \rho L \frac{g_l^{n+1,l-1} - g_l^n}{T^{n+1,l-1} - T^n} \,, & \text{if } T^{n+1,l-1} - T^n \neq 0 \,; \\ \rho C^{n+\frac{1}{2}} + \rho L \frac{1}{T_l - T_s} \,, & \text{if } T^{n+1,l-1} - T^n = 0 \\ & \text{and } T_s < T^n < T_l \,; \\ \rho C^{n+\frac{1}{2}} \,, & \text{otherwise.} \end{cases}$$

4. Solve for $\bar{T}$ the semi-discrete heat equation:

$$\hat{C}^{n+\frac{1}{2}} \frac{\bar{T} - T^n}{\Delta t} + \rho C^{n+\frac{1}{2}} (\mathbf{u}^n \cdot \nabla) \bar{T} - \nabla \cdot (k^{n+\frac{1}{2}} \nabla) \bar{T} = 0 \,, \quad (9)$$

with boundary condition at the interface with the sand mould of

$$-k^{n+\frac{1}{2}} \frac{\partial \bar{T}}{\partial n} = h^{n+\frac{1}{2}} (\bar{T} - T_{\text{sand}}) \,.$$

5. Define $T^{n+1,l}$ by under-relaxation, that is, take

$$T^{n+1,l} = \omega \bar{T} + (1 - \omega) T^{n+1,l-1} \quad \text{with} \quad 0 \leq \omega \leq 1 \,.$$

6. Test convergence: if

$$\frac{\| T^{n+1,l} - T^{n+1,l-1} \|_2}{\| T^{n+1,l} \|_2} \leq \epsilon \,,$$

stop iteration, and take $T^{n+1} = T^{n+1,l}$. Otherwise, set $l := l + 1$, go to step 2 and repeat steps 2–6.

A common practice in calculating the effect of latent heat is to use enthalpy. However, the calculation of enthalpy itself could be awkward if the properties are temperature dependent. Here at step 3, we use liquid fraction to calculate the latent heat effect instead of enthalpy. The advantage of doing so is that calculation of enthalpy is avoided.

# 4 Numerical results

We consider a representation of a TTF with a surrounding sand mould at the constant temperature $T_{\text{sand}} = 800°\text{C}$, and a constant heat transfer coefficient $h = 100\,\text{W}/(\text{m}^2°\text{C})$ at the outer boundary. The geometry is axi-symmetric with height of 205 mm, top radius of 25 mm and bottom radius of 50 mm (note that the bottom corner is smoothed out). A finite element mesh of 2842 six-node triangle elements with 5841 nodes and time steps of $\Delta t = 1\,\text{s}$ were used for the simulation. The computations were performed using the general purpose finite element package *Fastflo*. Other properties used are

$$\rho = 7000\,\text{kg/m}^3\,, \quad T_s = 1148\,°\text{C}\,, \quad T_l = 1156\,°\text{C}\,, \quad T_r = T_s\,,$$
$$\beta = 1\,\text{K}^{-1}\,, \quad L = 210\,\text{kJ/kg}\,, \quad K_o = 2000\,\text{s}^{-1}\,.$$

Viscosity $\nu$, conductivity $k$ and specific heat $C$ are piecewise linear functions of temperature interpolated between data points obtained from experiment. The actual values used are not included

TABLE 2: Temperature ranges and maximum speed of convection at different times during solidification. At each time, the topmost temperature range refers to the solution without convection.

| time (min) | min/max temp (°C) | max speed (mm/s) |
|---|---|---|
| 0 | 1400 - 1400 | - |
| | 1400 - 1400 | - |
| 5 | 1173 - 1297 | |
| | 1223 - 1272 | 13.27 |
| 10 | 1131 - 1188 | |
| | 1152 - 1168 | 12.25 |
| 15 | 1091 - 1156 | |
| | 1122 - 1156 | 1.42 |
| 20 | 1034 - 1156 | |
| | 1071 - 1156 | 1.59 |

here for reasons of confidentiality. The properties of the metal used in this example are typical of cast iron. The value of the permeability constant $K_o$ was taken from [3]. For comparison purposes, we repeated the calculations with and without convection. The numerical results show that without convection, solidification starts at $t = 5.6$ min; with convection, it starts later at $t = 9.2$ min. The field plots of temperature, liquid fraction and streamlines are shown in Figures 1–4 for t=5, 10, 15 and 20 min, respectively, and Table 2 gives a summary of the temperature ranges and flow speeds during solidification.

From the plots see that without convection, solidification progresses roughly uniformly along the entire boundary, with more rapid progression at the corners. With convection, early stage solidification is limited to the bottom region because convection brings cold liquid down the outer boundary and hot liquid up through the interior. As a result, the top region is kept hot longer than with-

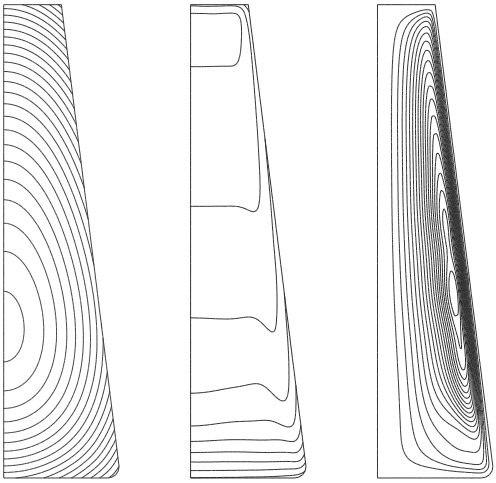

(a) (b) (c)

FIGURE 1: Solution at $t = 5$ min: (a) temperature field, conduction only, 5°C contour intervals; (b) temperature field with convection, 5°C contour intervals; (c) streamlines for convection. Solidification has not yet commenced.

out convection. Later, following the cooling of the liquid in the whole casting region, convection dies down, the stratification disappears and the temperature field resembles that of the conduction only case. The final point of solidification is slightly higher for the convection solution, due to the initial vertical stratification. The effect of latent heat is clearly seen in the 15 and 20 minute solutions, where there is a significant region held at the liquidus temperature. Note also that the temperature range is always smaller for the convection solution.

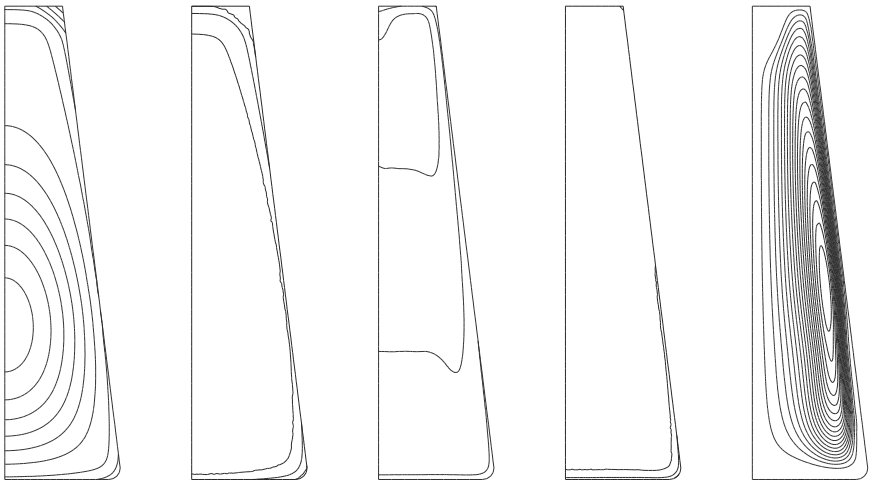

(a) (b) (c) (d) (e)

FIGURE 2: Solution at $t = 10$ min: (a) temperature field, conduction only, 5°C contour intervals; (b) liquid fraction contours at $g_l = 0.01$, 0.5, 0.99, conduction only; (c) temperature field with convection, 5°C contour intervals; (d) liquid fraction contours at $g_l = 0.01$, 0.5, 0.99, with convection; (e) streamlines for convection.

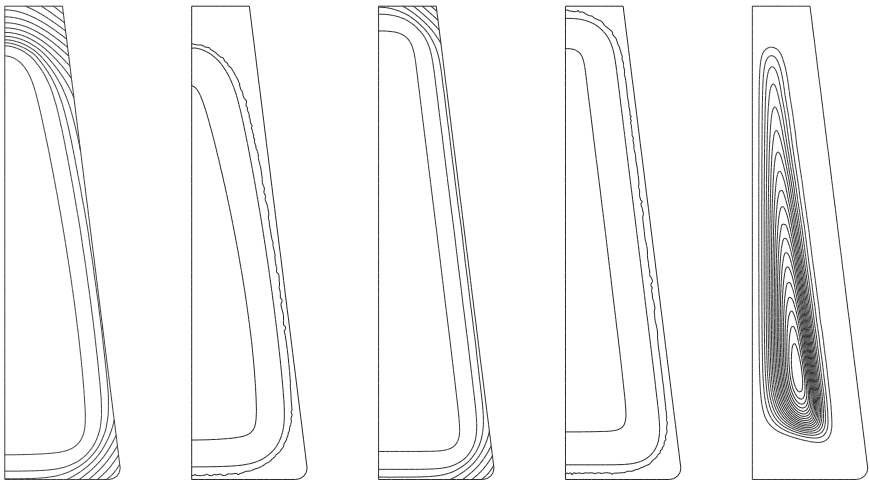

(a) (b) (c) (d) (e)

FIGURE 3: Solution at $t = 15$ min: (a) temperature field, conduction only, 5°C contour intervals; (b) liquid fraction contours at $g_l = 0.01$, 0.5, 0.99, conduction only; (c) temperature field with convection, 5°C contour intervals; (d) liquid fraction contours at $g_l = 0.01$, 0.5, 0.99, with convection; (e) streamlines for convection.

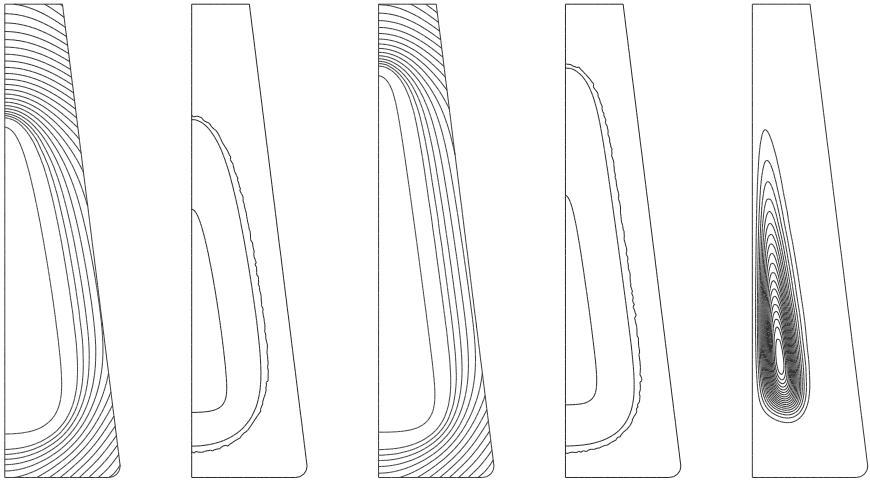

(a) (b) (c) (d) (e)

FIGURE 4: Solution at $t = 20$ min: (a) temperature field, conduction only, 5°C contour intervals; (b) liquid fraction contours at $g_l = 0.01$, 0.5, 0.99, conduction only; (c) temperature field with convection, 5°C contour intervals; (d) liquid fraction contours at $g_l = 0.01$, 0.5, 0.99, with convection; (e) streamlines for convection.

The velocity field, represented by the streamline plots in the figures, show a rapid acceleration from a quiescent initial condition to a maximum after a few minutes, is maintained until significant solidification occurs, then decays relatively quickly. The form of the Darcy coefficient $\tilde{K}$ is such that the effect of the mushy layer on the flow is small except near the solidification end. In order to obtain stable solutions, some streamline upwinding and, at times, numerical diffusion, were added to the solutions. The amounts added were relatively small, and should not affect the overall form of the solution.

In terms of the significance of natural convection in the TTF, its main effect is likely to be the delay in the freezing of the top surface due to the stratification. As soldification progresses and the TTF loses fluid due to shrinkage in an accompanying casting, the top surface of the TTF will drop, if it remains liquid for a sufficient time. As a consequence, the heat loss at the top may be reduced, thus prolonging the solidification even further. In this way, natural convection is an aid to the operation of a TTF.

# 5 Conclusions

The numerical tests show that the computer model for solidification with convection developed in this work is a useful tool for improved understanding of the behaviour of TTFs. Some fine tuning of parameters controlling the solution process is needed for some relatively more difficult situation, particularly as the speed of the convective flow increases. Turbulence is not included in this model, however, by applying a small amount of streamline upwinding or artificial diffusion, certain near turbulent cases can still be simulated.

The numerical results show clearly the well known fact that con-

vection will have a dominant effect during the early period of solidification. Convection will retard the onset of solidification. This occurs, even though the heat flux out of the casting is higher than that due to conduction alone, and is due to the reduction in thermal gradients in the bulk caused by the convective motion. Also due to convection, the effect of stratification is positive for the operation of a TTF, since the top region is kept hot longer, and solidification will occur first at the bottom of a TTF. In a real TTF, molten iron is lost to a casting, so the volume of liquid in the TTF is reducing. Because of the stratification, the top surface solidifies latest, and so the melt level drops, forming a gap between the liquid metal and the sand mould. This in turn may affect the heat loss at the top of the TTF, further enhancing the stratification effect. At this stage, we have no simple means of accommodating the effect of the top surface falling, but it is worth considering as a topic for future investigation.

The results here are only representative of the real situation. They do not properly account for heat transfer, predominantly by conduction, in the sand mould, nor do they account for three dimensional effects due to flow from the TTF into (usually more than one) casting. We have further developed the model to include the former effect, and the latter is likely to be principally a matter of using sufficient computer resources to obtain accurate solutions. In addition, the effects of shrinkage and surface deformation mentioned above should be addressed.

**Acknowledgements:** we thank Dr Dayalan Gunasegaram of the Toowoomba Foundry, for his interest in this work, and for supplying data on the properties of cast iron.

# References

[1] J. H. Chen, H. L. Tsai, An Efficient and Accurate Numerical Algorithm for Multi-Dimensional Modelling of Casting Solidification, Part I: Control Volume Method *Transactions of the American Foundrymen's Society*, **98**, pp.527–537 (1990). C497

[2] R. W. Lewis, K. Ravindran, Finite Element Simulation of Metal Casting *Int. J. Numer. Meth. Engng*, **47**, pp.29–59 (2000). C497, C499

[3] V. R. Voller, A. D. Brent, C. Prakash, Modelling the Mushy Region in a Binary Alloy *Appl. Math. Modelling*, **14**, pp.320–326 (1990). C499, C500, C504

[4] V. R. Voller, C. R. Swaminathan, Fixed Grid Techniques for Phase Change Problems: A Review *Int. J. Numer. Meth. Engng*, **30**, pp.000–023 (1990). C499

[5] M. J. Voss, H. L. Tsai, Effects of the Rate of Latent Heat Release on Fluid Flow and Solidification patterns During Alloy Solidification *Int. J. Engng Sci.*, **34**, No. 6, pp.715–737 (1996). C499

[6] X. K. Lan, J. M. Khodadadi, Fluid Flow, Heat Transfer and Solidification in the Mold of Continuous Casters During Ladle Change *Int. J. Heat Mass Transfer*, **44**, pp.953–965 (2001). C499

[7] C. H. Li, R. Glowinski, Modelling and Numerical Simulation of Low-Mach-Number Compressible Flows *Int. J. Numer. Meth. in Fluids*, **23**, pp.77–103 (1996). C501